

## Supplementary Information:

### Amorphized ZnSb-based composite anodes for high-performance Li-ion batteries

Min-Gu Park<sup>a</sup>, and Churl Kyoung Lee<sup>a</sup>, Cheol-Min Park<sup>\*a</sup>

<sup>a</sup>School of Advanced Materials and System Engineering, Kumoh National Institute of Technology, Gumi, Gyeongbuk 730-701, Korea.

#### Experimental

**Materials Synthesis:** Amorphized ZnSb/MgO/C and ZnSb/Al<sub>2</sub>O<sub>3</sub>/C composites were synthesized by the following processes. ZnO (Kojundo, 99.5%, 10 μm), Sb<sub>2</sub>O<sub>3</sub> (Aldrich, 99%, 5 μm), amorphous carbon (Super P), Mg (Daejung, 99%, 100 μm) or Al (Daejung, 99%, 100 μm), and stainless steel balls (diameter: 3/8 in. and 3/16 in.) were put into a hardened steel vial (80 cm<sup>3</sup>) with a ball-to-powder ratio of 20:1. For the complete mechanochemical reduction reactions to take place, as shown in Eqs. (3) and (4), the molar ratios of the ZnO/Sb<sub>2</sub>O<sub>3</sub>/Mg and ZnO/Sb<sub>2</sub>O<sub>3</sub>/Al powders were set to 2:1:5 and 6:3:10, respectively. The high-energy mechanical milling (HEMM) process (Spex-8000) was conducted under an Ar atmosphere for 6 h. Preliminary studies on the electrochemical performance also showed that the optimum amounts of ZnO/Sb<sub>2</sub>O<sub>3</sub>/Mg (or ZnO/Sb<sub>2</sub>O<sub>3</sub>/Al) and C were 70 and 30 wt%, respectively. In addition, the amounts of crystalline MgO and amorphous Al<sub>2</sub>O<sub>3</sub> in the ZnSb/MO<sub>x</sub>/C composites were estimated to be approximately 24.4 and 21.8 wt%, respectively.

**Materials Characterization:** Amorphized ZnSb/MgO/C and ZnSb/Al<sub>2</sub>O<sub>3</sub>/C composites were identified by X-ray diffraction (XRD, D-MAX2500-PC, Rigaku), X-ray photoelectron spectroscopy (XPS, AXIS, Kratos), and high-resolution transmission electron microscopy (HRTEM, Tecnai G2 F20 S-TWIN, FEI) operated at 200 kV. For the TEM analysis, a dilute suspension was dropped on a carbon-coated TEM grid and dried.

**Electrochemical Measurements:** For electrochemical evaluation of Zn, Sb, ZnSb, the ZnSb/MgO/C composite, and the ZnSb/Al<sub>2</sub>O<sub>3</sub>/C composite, electrodes were prepared by coating slurries containing the active material (70 wt%), carbon black (Denka, 15 wt%) as a conductor and polyvinylidene fluoride dissolved in n-methyl pyrrolidinone as a binder (15 wt%) on copper foil substrates, followed by drying at 120 °C for 4 h under vacuum. Coin-type electrochemical cells were assembled in an Ar-filled glove box using Celgard 2400 as a separator, Li foil as the counter and reference electrodes, and 1 M LiPF<sub>6</sub> in ethylene carbonate/diethyl carbonate [1:1 (v/v), Panax Starlyte] as an electrolyte. All of the cells were galvanostatically tested between 0.0–2.0 V (vs. Li/Li<sup>+</sup>) at a current density of 100 mA g<sup>-1</sup> using a Maccor automated tester, except for the rate capability tests. The gravimetric capacity was calculated with respect to all the active elements (such as ZnSb and C), whereas the volumetric capacity was obtained from the gravimetric capacity by multiplying the density of ZnSb (6.4 g cm<sup>-3</sup>) by its weight percent. Lithium was inserted into the electrode during the discharge reaction and was extracted from the working electrode during the charge reaction.

## Results

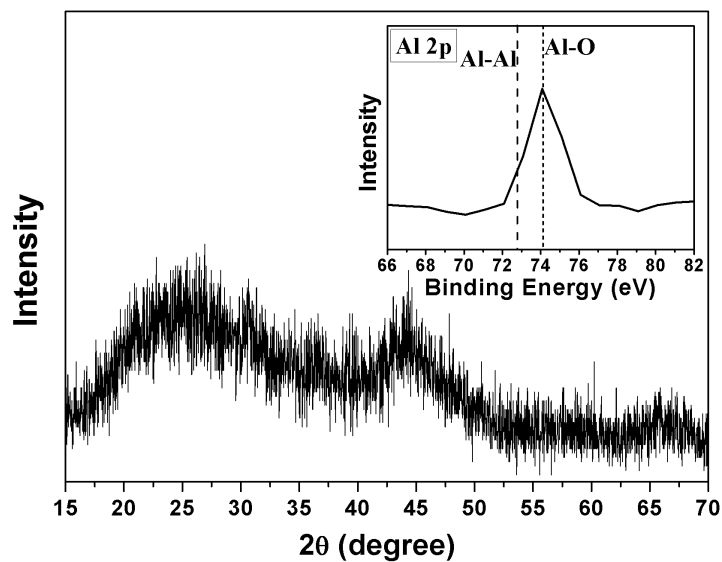
Figure S1(a) shows the XRD pattern of the ZnSb/Al<sub>2</sub>O<sub>3</sub>/C composite synthesized by the hybrid mechanochemical reduction. The XRD peaks are broad, which demonstrates that the ZnSb/Al<sub>2</sub>O<sub>3</sub>/C composite was amorphized. XPS analysis of the ZnSb/Al<sub>2</sub>O<sub>3</sub>/C composite detected amorphous Al<sub>2</sub>O<sub>3</sub> (2p: 74.1 eV), as shown in the inset of Fig. S1(a). Figure S1(b) shows TEM bright-field and HRTEM images combined with selected area diffraction patterns of the ZnSb/Al<sub>2</sub>O<sub>3</sub>/C composite. The HRTEM image shows less than 3 nm-sized amorphized ZnSb and amorphous Al<sub>2</sub>O<sub>3</sub> were well dispersed within the amorphous carbon matrix. Additionally, the EDS mapping images confirm that ZnSb, Al<sub>2</sub>O<sub>3</sub>, and carbon were well dispersed within the composite.

Figure S2(a) shows the electrochemical characteristics of the ZnSb/Al<sub>2</sub>O<sub>3</sub>/C composite electrode. The synthesized ZnSb/Al<sub>2</sub>O<sub>3</sub>/C composite electrode showed high initial discharge/charge capacities of 642/479 mAh g<sup>-1</sup> (ca. 1980/1478 mAh cm<sup>-3</sup>), with a relatively high initial coulombic efficiency of 74.6%. Figure S2(b) shows the differential capacity plots of the first cycle for the ZnSb and ZnSb/Al<sub>2</sub>O<sub>3</sub>/C composite electrodes. All the peaks are well matched for the same reaction potential, which suggests that these electrodes were involved in the three electrochemical reactions mentioned in the manuscript, a result which is in good agreement with the results of our previous ZnSb-related study.

Figures S3(a) and (b) show the electrochemical characteristics of the Zn and Sb electrodes, respectively. The Zn electrode showed initial discharge/charge capacities of 413/206 mAh g<sup>-1</sup>, with a poor initial coulombic efficiency of 49.9%. The capacity retention after the 10th cycle was ca. 84% of the first charge capacity. The Sb electrode showed initial discharge/charge capacities of 723/627 mAh g<sup>-1</sup>, with a good initial coulombic efficiency of 86.7%. However, the capacity retention of the Sb electrode after the 10th cycle was ca. 40.5% of the first charge capacity. The poor electrochemical behaviors of the Zn and Sb electrodes were caused by the large volume change that occurred during formation of the LiZn and Li<sub>3</sub>Sb phases, respectively, associated with the pulverization of the active material and its electrical isolation from the current collector.

## Figures

(a)



(b)

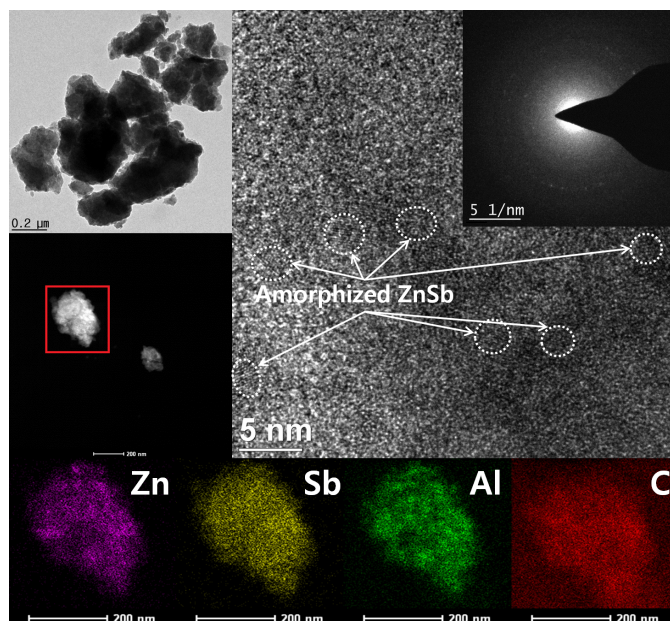
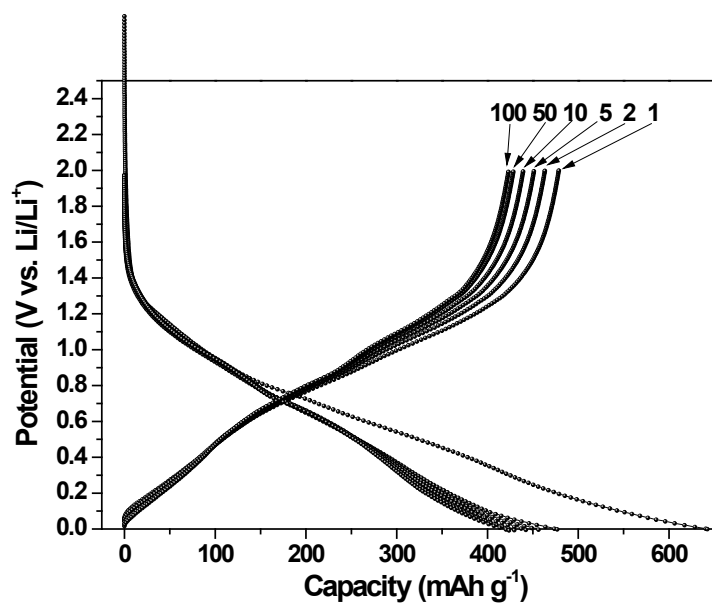


**Figure S1. Characterization of ZnSb/MgO/C composite: (a) XRD pattern and XPS results and (b) bright-field TEM and HRTEM with corresponding lattice spacing and EDS mapping images of ZnSb/MgO/C.**

(a)



(b)

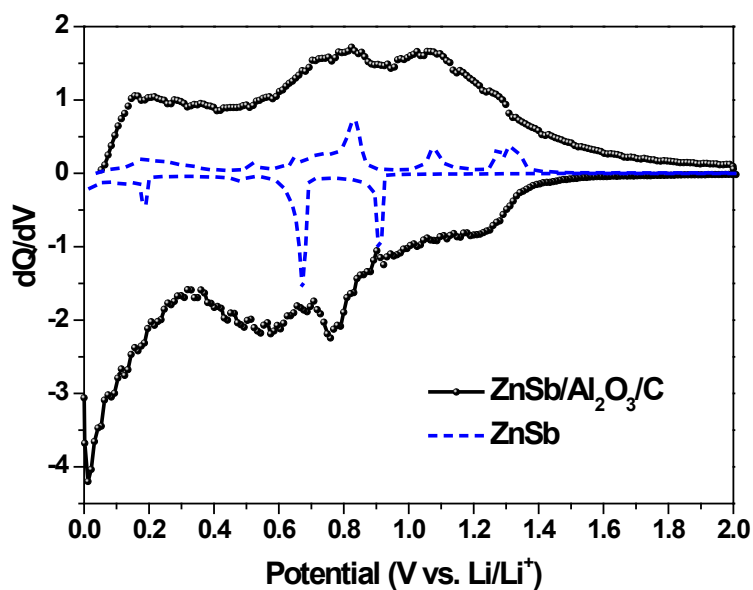
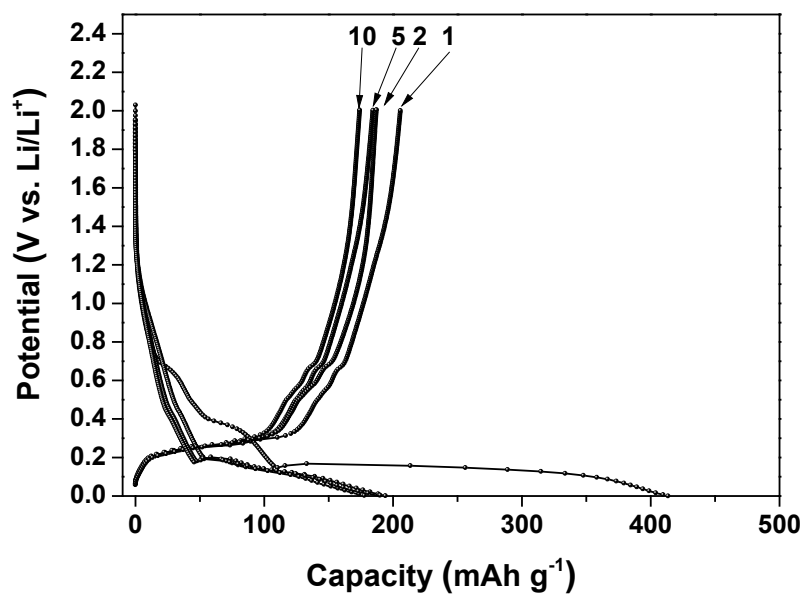


**Figure S2. Electrochemical characteristics of ZnSb/MgO/C composite electrode:** (a) Voltage profile of ZnSb/MgO/C composite electrode (current rate:  $100 \text{ mA g}^{-1}$ , voltage window: 0–2.0 V) and (b) DCP results for the first cycle of ZnSb and ZnSb/MgO/C composite electrodes.

(a)



(b)

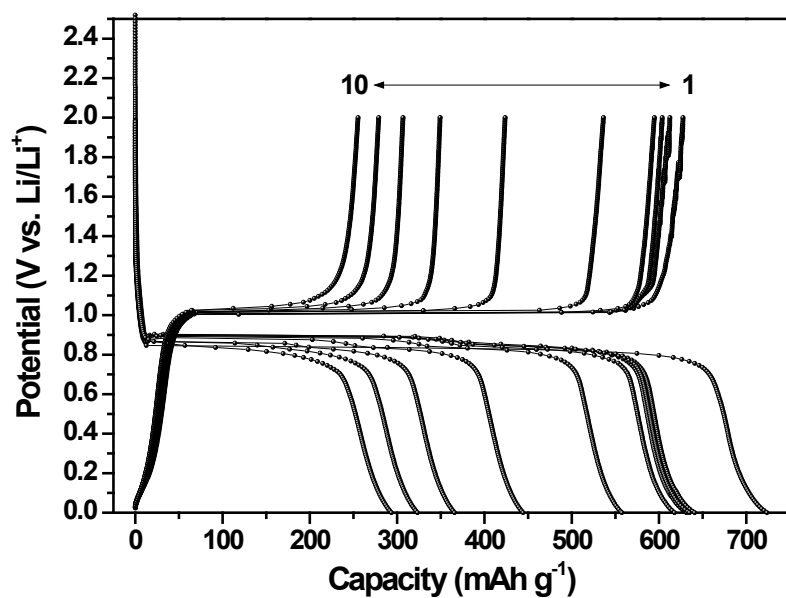


**Figure S3. Electrochemical characteristics of Zn and Sb electrodes:** (a) Voltage profile of Zn electrode and (b) voltage profile of Sb electrode (current rate: 100 mA g<sup>-1</sup>, voltage window: 0–2.0 V).